Video Article

High-resolution Optical Mapping of the Mouse Sino-atrial Node

Di Lang[1], Alexey V. Glukhov[1]

[1]Department of Medicine, University of Wisconsin-Madison School of Medicine and Public Health

Correspondence to: Alexey V. Glukhov at aglukhov@medicine.wisc.edu

URL: https://www.jove.com/video/54773
DOI: doi:10.3791/54773

Keywords: Biophysics, Issue 118, optical mapping, sino-atrial node, mouse, heart, action potential

Date Published: 12/2/2016

Citation: Lang, D., Glukhov, A.V. High-resolution Optical Mapping of the Mouse Sino-atrial Node. *J. Vis. Exp.* (118), e54773, doi:10.3791/54773 (2016).

Abstract

Sino-atrial node (SAN) dysfunctions and associated complications constitute important causes of morbidity in patients with cardiac diseases. The development of novel pharmacological therapies to cure these patients relies on the thorough understanding of both normal physiology and pathophysiology of the SAN. Among the studies of cardiac pacemaking, the mouse SAN is widely used due to its feasibility for modifications in the expression of different genes that encode SAN ion channels or calcium handling proteins. Emerging evidence from electrophysiological and histological studies has also proved the representativeness and similarity of the mouse SAN structure and functions to larger mammals, including the presence of specialized conduction pathways from the SAN to the atrium and a complex pacemakers' hierarchy within the SAN. Recently, the technique of optical mapping has greatly facilitated the exploration and investigation of the origin of excitation and conduction within and from the mouse SAN, which in turn has extended the understanding of the SAN and benefited clinical treatments of SAN dysfunction associated diseases. In this manuscript, we have described in detail how to perform the optical mapping of the mouse SAN from the intact, Langendorff-perfused heart and from the isolated atrial preparation. This protocol is a useful tool to enhance the understanding of mouse SAN physiology and pathophysiology.

Video Link

The video component of this article can be found at https://www.jove.com/video/54773/

Introduction

Novel scientific breakthroughs that lead to leaps in the understanding of human physiology are often preceded by technological advances. Fluorescent optical mapping, for example, enables investigation of multiple physiological parameters in both cells and tissues.[1,2] It significantly improved our understanding of how the anatomical structure is associated with electrophysiological functions and dysfunctions. In the heart, the natural pacemaker and conduction systems such as the sinoatrial node (SAN) and the atrioventricular junction consist of nodal myocytes that are insulated by the surrounding atrial myocytes.[3-5] Such organization creates complex three-dimensional structures with specialized electrical properties. Both structural and functional remodeling of these pacemaker structures has been recognized to form significant electrophysiological heterogeneities.[6,7] Understanding the mechanism underlying how such heterogeneities result in SAN dysfunctions and atrial arrhythmogenesis will dramatically benefit the clinical treatment of these diseases. It requires a technique to visualize the propagation of electrical signals at the tissue level, such as optical mapping.

Recently, accumulating evidence has proven the advance of optical mapping in studies of atrial electrophysiology and pathology.[2] However, novel and rigorous studies are dependent on the accurate interpretation of experimental data, whose validity and stability rely on careful experiment protocols. Genetically modified mice are extensively used for research as animal models of human diseases including sick sinus syndrome, pacemaker abnormalities and atrial arrhythmias.[6,8-11] Thus, a combination of fluorescent optical mapping with transgenic mouse models provides a powerful tool to study cardiac electrical abnormalities associated with various pathologies. In this paper, we present a protocol for high-resolution optical mapping of the mouse SAN and atrium. Specifically, we discuss and compare different dye loading approaches, time effects on dye bleaching and heart rate stability during the experiment.

Protocol

All experiments were conducted in accordance with the National Institutes of Health Guide for the Care and Use of Laboratory Animals (NIH Pub. No. 80-23). All methods and protocols used in these studies have been approved by The University of Wisconsin Animal Care and Use Protocol Committee following the Guidelines for Care and Use of Laboratory Animals published by NIH (publication No. 85-23, revised 1996). All animals used in this study received humane care in compliance with the Guide for the Care and Use of Laboratory Animals.

1. Heart Removal and Langendorff Perfusion

1. Prior to heart isolation, warm Tyrode solution to 37 °C by using a water bath and a water jacket.

2. Anesthetize the mouse with 5% isoflurane/95% O_2.
3. Ensure appropriate level of anesthesia by checking the loss of pain reflex.
4. Perform thoracotomy. Open the chest by using curved 5.5" Mayo scissors and 5.5" Kelly hemostatic forceps to make a 1 cm cut on the front of the thorax.
    1. Quickly extract the heart from the chest (within 30 sec). Use 4" curved Iris forceps to grab the lung tissue and cut out the lung, thymus and heart together with the pericardium using 4.3" Iris scissors. Do not grab the heart directly.
    2. Wash it in oxygenated (95% O_2 / 5% CO_2), constant-temperature (36.8 ± 0.4°C) modified Tyrode's solution. Use the following solution composition (in mM): 128.2 NaCl, 4.7 KCl, 1.19 NaH_2PO_4, 1.05 $MgCl_2$, 1.3 $CaCl_2$, 20.0 $NaHCO_3$, and 11.1 glucose (pH 7.35 ± 0.05).
5. While bathed in the same solution, identify the lung, thymus, and fat tissue. Carefully dissect them from the heart. Use curved 3" Vannas-Tubingen scissors and 4.3" #5 forceps.
6. Then identify the aorta and cannulate it onto a custom-made 21 G cannula. Use two curved 4.3" #5B forceps.
7. After cannulation, simultaneously perfuse (through the cannula at a flow rate of ~5 ml/min; this should be adjusted based on the aortic pressure, see below) and superfuse (in the bath at a flow rate of ~50 ml/min) the heart with warmed and filtered Tyrode solution throughout the entire experiment. Pass the perfusion solution through an in-line 11 µm nylon filter to prevent clogging of coronary circulation.
8. Using a pressure transducer (or a pressure gauge) connected via a 3-way stopcock Luer lock to the perfusion line, monitor the aortic pressure and maintain it between 60 and 80 mmHg. Adjust perfusion speed if required to keep the aortic pressure within this range.

2. Optical Mapping of the SAN from the Langendorff-perfused Whole Heart

1. **Instrumentation**
    1. Place the heart horizontally and pin the ventricular apex to the silicon-coated bottom of the chamber using 0.1 mm diameter pins to prevent stream-induced movement during the experiment.[12]
    2. Insert a small (.012" I.D. x .005") silicon tube into the left ventricle (LV) via the pulmonary vein, the left atria (LA) and the mitral valve (MV). Fix the tube by a silk suture (4-0) to the sounding connective tissue.
    3. Position the heart with its posterior side facing up (**Figure 1A**, *left panel*).
    4. Pin the edge of the RA appendage (RAA) to the silicon bottom of the chamber using 0.1 mm diameter minutien pins. Adjust its level in order to make the posterior surface of the RA flat and allow it to be located the camera's focal plane. This will enable optical measurements from the maximal surface area of the atrium.
    5. Noose superior (SVC) and inferior (IVC) vena cava by a silk suture (4-0), stretch and pin the other end of the suture to the bottom of a silicon-coated chamber (see **Figure 3A**). Make sure the sutures do not block the optical field of view.
    6. Place the custom-made pacing electrode on the edge of the RAA. To make electrodes, use silicon coated 0.25 mm diameter silver wires, with 0.5 mm inter-electrode distance and devoid of silicon for a length of 1 mm at the pacing end. Then place two ECG 12 mm needle (29-gauge) monopolar electrodes near the base of the right and left ventricles. Place the ground ECG electrode near the apex of the ventricles .
2. **Staining**
    1. Since both fluorescent dyes and electro-mechanical uncoupler blebbistatin are light-sensitive, perform all the procedures described below in a dark room. First prepare voltage-sensitive dye RH-237 or di-4-ANNEPS as a stock solution, 1.25 mg/ml in dimethyl sulfoxide (2.5 mM), aliquot it (30 µl each) and store the aliquots at -20 °C.
    2. Dilute 5-10 µl of dye stock solution in 1 ml of warmed (37 °C) Tyrode solution and then inject it into the coronary perfusion line over a period of 5-7 min using an in-line Luer injection port.
    3. Prepare blebbistatin as a stock solution (2 mg/ml in dimethyl sulfoxide, 6.8 mM) in advance and store it at 4°C.
    4. After 20 min of stabilization, add 0.5 ml of warmed (37 °C) blebbistatin in the perfusate and dilute 0.1 ml of blebbistatin in 1 ml of warmed (37 °C) Tyrode solution. Then inject into the coronary perfusion line over a period of 5-7 min using an in-line Luer injection port.

3. Optical mapping of the SAN from the Isolated Atrial Preparation

1. **Instrumentation**
    1. For the isolated atrial preparation, isolate and cannulate the heart as described above in steps 1.1-1.5 for whole-heart preparation.
    2. Dissect the ventricles away from the anterior side. See **Figure 1A**, *right panel*, *cut #1* for details.
    3. Open the RA by cutting through the tricuspid valve (TV) along the TV-SVC axis. See **Figure 1A**, *right panel*, *cut #2* for details.
    4. Cut the medial limb of the crista terminalis to open the RAA. See **Figure 1A**, *right panel, cut #3*.
    5. Open the anterior atrial free wall by performing a cut from the midline of the previous cut#3 to the edge of the right bottom corner of the RAA, flatten and pin the atrial free wall to the bottom of a silicon-coated chamber. See the direction shown by the hollow arrow in **Figure 1A**, *cut #4*. Preserve a rim of ventricular tissue for pinning the preparation to prevent damage to the atria.
    6. Similarly, open LA by cutting through the MV along the MV-upper corner of the LA appendage (LAA).
    7. To open the LAA, cut from the middle of the opened LAA, through the anterior atrial free wall until near a middle rim of the LAA.
    8. Open the anterior atrial free wall along the same direction, then flatten and pin it to the bottom of a Sylgard-coated chamber.
    9. Partially remove the interatrial septal tissue. This will reduce scattering of the optical signal from tissue that is not in focus. Therefore, both the LA and RA as well as the SAN and atrio-ventricular junction (AVJ) are accessible in this preparation (**Figure 1B**).
    10. Lift up the final preparation by about 0.5 mm from the bottom of the silicon-coated chamber in order to allow superfusion from both epicardial and endocardial surfaces.
    11. Superfuse the preparation with warmed (37 °C) Tyrode solution at a constant rate of ~12 ml/min for a focused flow located near the SVC and ~30 ml/min for a bath superfusion.
    12. Place the custom-made pacing Ag/$AgCl_2$ electrode (0.25 mm diameter) on the edge of the dissected RAA. Then place two ECG 12 mm needle (29G) electrodes (monopolar) near the RAA and LAA, respectively. Place the ground ECG electrode near the AVJ.

2. **Staining**
    1. Perform a direct application of the voltage-sensitive dye (RH-237 or di-4-ANNEPS). For this, dilute 1-2 µl of the dye stock solution in 1 mm of warmed (37 °C) Tyrode solution and slowly release the diluted dye on the surface of the preparation by using a 1 mm pipette.
    2. Alternatively, perform atrial staining with the voltage-sensitive dye through a coronary perfusion of the Langendorff-perfused heart similar to that described above for the whole-heart preparation (steps 2.2.1-2.2.2).
        1. After the coronary perfusion staining, isolate the atrial preparation as described. Perform additional surface staining when needed to reach a satisfactory fluorescence level. Quick atrial isolation does not bleach the dye and does not affect the quality of staining.
    3. Immobilize the preparation with the electro-mechanical uncoupler, blebbistatin. Dilute 3-5 µl blebbistatin stock solution in the warmed (37 °C) Tyrode solution and slowly release the diluted blebbistatin on the surface of the preparation and surrounding solution. Since blebbistatin has been shown to be light sensitive,[13,14] avoid long exposure to light during preparation and staining.
    4. Perform additional blebbistatin application as much as needed to suppress contraction. Normally up to 3 additional applications (3-5 µl per each application) can be used to suppress the motion artifact sufficiently in order to accurately reconstruct SAN and atrial activation.
    5. Add additional 0.5 ml of warmed blebbistatin in the perfusate. During this procedure, pause the superfusion for 30 sec to allow the dye/blebbistatin to stain the atrial tissue.

4. Optical Mapping Set Up

NOTE: A detailed description of the optical mapping system is provided elsewhere.[12]

1. Use a camera with a temporal resolution of 2,000 frames/sec or higher, and a series of condenser lenses to reach spatial resolution of 100 µm/pixel or higher. This is required to reconstruct SAN activation and intranodal propagation.
2. To reduce motion artifact from the vibrating solution, fix a small cover glass on the surface of the solution over the heart/isolated atrial preparation.
3. Use excitation light (520 ± 45 nm wavelength) provided by a constant-current, low-noise halogen lamp. Direct the filtered light beam onto the preparation by using a flexible bifurcated light guide.
4. Filter the emitted fluorescence by a long-pass filter (>715 nm). Collect, digitize and save the acquired fluorescent signal on a computer using software provided by the camera manufacturer.

5. Data Processing

NOTE: Optical mapping data is collected and stored as a series of matrices of fluorescent intensity at different time points. Each pixel represents a measure of fluorescent intensity collected from a specific location on the tissue preparation at a specific time point. Background fluorescence is automatically removed per pixel to allow for better visualization of fluorescence changes produced by membrane voltage changes and inverted to correspond with action potentials (APs) measured by microelectrode systems. Details of the different steps in processing optical imaging data, including image segmentation, spatial filtering, temporal filtering, and baseline drift removal, are provided in the focused review.[15]

1. Manually or by using the special algorithm (for example, a thresholding or edge detection)[15] to determine tissue boundaries, create a binary mask of 1 (included pixels) and 0 (excluded pixels) and apply the mask to each frame in the sequence. This process creates a binary image that highlights areas of interest for further processing.
2. To improve signal-to-noise ratio of the optical data, filter the signals within the selected areas of interest. For this, use spatial (*i.e.* averaging of neighboring fluorescent pixels as defined by a desired convolution bin or kernel, for instance 3 x 3 or, for noisy data, 5 x 5) and/or temporal filtering (for example, Butterworth, Chebyshev type 1, Chebyshev type 2, Elliptic *etc.*) (**Figure 2**). Keep in mind the possibility of filtered-induced artifacts when interpreting the data. For more details, see review.[15]
3. Remove drift of baseline in optical recordings when needed (by using high-pass filtering or polynomial fitting to the original signal) and then normalize each pixel signal from 0 (minimum fluorescence) to 1 (maximum fluorescence).
4. Select a time window that encompasses the activation times of all the pixels for a single AP propagation. Assign each pixel its activation time as the time of maximum upstroke derivative (dF/dt_{max}, where F is fluorescence intensity). Using all pixel activation times, reconstruct the isochronal activation map. Each isochron will thus show the pixels activated at the same time.
5. To reconstruct the AP duration (APD) distribution map, for each pixel calculate the duration between the activation time and the time at a specific level of repolarization (for example, at 80% of repolarization, APD_{80}). Using all pixel APD values, reconstruct the APD distribution isochronal map. Each isochron will thus show the pixels with the same APD.
6. To calculate conduction velocity for AP propagation, fit a surface of the preparation to the activation time data calculated in 5.4. For this, use polynomial surface fitting or local kernel surface smoothing and then calculate local conduction velocity vectors from the gradient of the fitted surface.
7. To create the repolarization map, assign each pixel its repolarization time, defined as the maximum second derivative (d^2F/dt^2) of the optical signal at the end of the OAP, or the time of 90% repolarization.

Representative Results

Optical Mapping of the Intact SAN from the Langendorff-perfused Heart

A typical example of an RA activation contour map reconstructed for spontaneous sinus rhythm is shown in **Figure 3** for a Langendorff-perfused mouse heart. The early activation point is located within the intercaval region near the SVC where the SAN is anatomically defined.[3,16] Two RA activation contour maps acquired at 1.0 and 0.5 msec sampling rate are shown in **Figure 3B**.

To evaluate SAN functioning, we measured the SAN recovery time (SANRT).[9] After RAA pacing for at least 1 min at 10-12 Hz, the electrical stimulation was stopped and SANRT was calculated as the time interval between the last captured AP and the first spontaneous AP (**Figure 3C**). The SANRT was corrected to the heart rate (*i.e.* $SANRT_c$) by calculating the difference between the SANRT and the basis cycle length. In addition, the location of the first post-pacing pacemaker was identified. For this example, the SANRTc was about 49 msec.

Isolated Atria and SAN Activation

The activation of the isolated atrial preparation during spontaneous sinus rhythm is shown in **Figure 4A**. It originated in the anatomically defined SAN near the SVC with a wide wave front that spread anisotropically throughout the RA, with two preferential conduction directions near the superior and inferior SAN edges and complete block to the septal direction (marked in activation maps in **Figure 4A**). The activation map acquired at 1 msec sampling rate shows an extensive area of early activation. An increase in the sampling rate to 0.5 msec and 0.3 msec allows us to identify the precise area of the leading pacemaker location. We observed a typical, beat-to-beat stable monofocal position of the leading pacemaker which corresponded to the primary pacemaker area previously characterized electrophysiologically by glass microelectrodes[17] and optical mapping[8-11,18,19] as well as by immunolabeling for connexin45 and HCN4.[6,16]

As demonstrated previously, the SAN optical action potential consists of a two-phase signal which includes two distinct components: the slowly rising SAN component and the rapidly rising upstroke of the atrial myocardium (atrial component) (**Figure 4B**).[20] Because of light scattering processes, OAP represents an averaged electric activity arising from multiple layers of cells within the tissue. The scattering depth and width is governed by a space constant, which is determined by light scattering and absorption properties and can reach up to 1.5-2 mm. Because of the SAN conduction delay, the SAN AP always precedes atrial activity during physiological activation (**Figure 4B**). To calculate the transition from the SAN to the atrium (*i.e.* SAN conduction time, SANCT), we used either the time point where the double-component SAN signal reaches 50% of the SAN component amplitude, or the first peak of the two-peak OAP first derivative (dF/dt). The SANCT from the area of earliest SAN activation to the RA was ~5 msec, similar to that measured by glass microelectrodes.

SAN Recovery Time

Similarly, the SANRT was measured in the isolated atrial preparation (**Figure 4D**). For this, atrial preparations were paced at 12 Hz through a pacing electrode located at the corner of the RAA for at least 1 min.[9] For this example, the SANRTc was about 34 msec, which is comparable with that measured in the Langendorff-perfused heart (**Figure 3C**). In addition, the location of the first post-pacing pacemaker was identified.

Heart Rhythm and Fluorescent Signal Stability Over Time

If the surgery and dye loading procedures are followed appropriately, there should not be any significant change in the physiological characteristics of the atrium. In **Figure 5**, we present the heart rhythm measured before and after the atrial isolation procedure and during the 3 hr perfusion. No significant changes of heart rate were observed either during atrium isolation or after dye loading.

Although arterial staining may require a larger amount of dye, the stability of the fluorescent signal in the SAN area tissue appears to be better by using this loading method. In **Figure 6**, we present signal intensity decay over time for both coronary and surface staining. In the SAN tissue, IC_{50} (which indicates the period when signal intensity has deceased to 50%) is about 107 min after coronary staining, almost twice as long as that of surface staining.

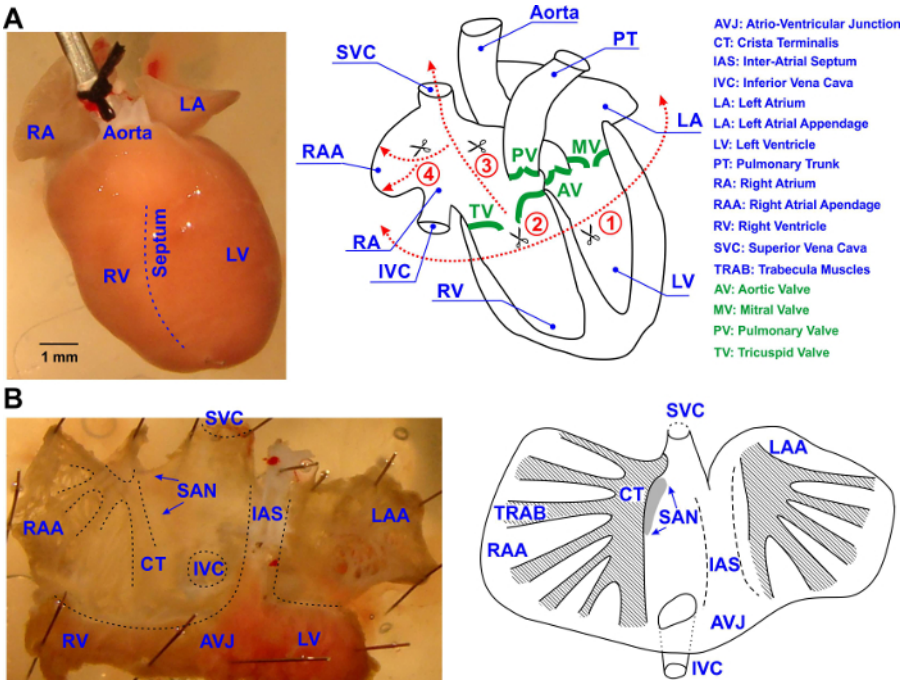

Figure 1: Isolation of the Mouse Atrial Preparation. (**A**) Surgical procedures performed to isolate mouse atrial preparation. The posterior view of the heart is shown. All cuts are shown by dotted red lines and labeled by numbers in the order performed. See details in text. (**B**) The schematic outline of the isolated mouse atrial preparation showing the main anatomical features, including the trabecular structure of the left and right atrial appendages as well as the location of the sino-atrial node (SAN; labelled by a grey oval). All abbreviations are explained in the figure. Please click here to view a larger version of this figure.

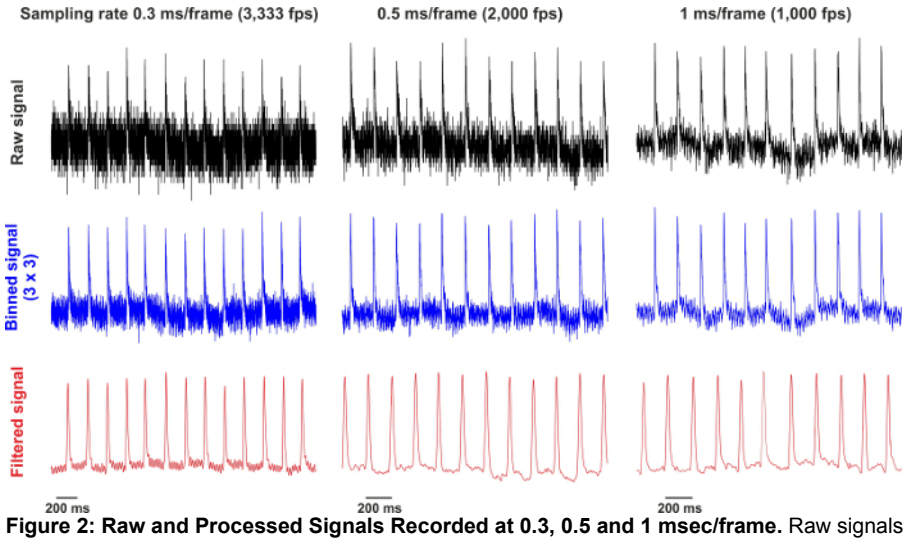

Figure 2: Raw and Processed Signals Recorded at 0.3, 0.5 and 1 msec/frame. Raw signals are collected from a single pixel. After 3 x 3 binning, the signals are filtered by using the low-pass Butterworth algorithm. Please click here to view a larger version of this figure.

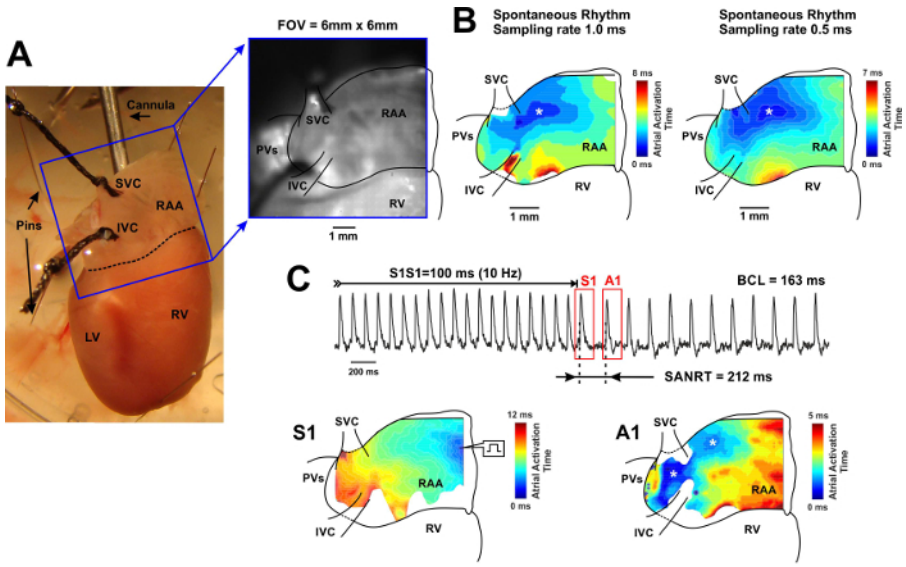

Figure 3: Whole-heart Optical Mapping of the SAN. (**A**) *Left,* photo of a typical preparation used for the mapping of the SAN from the intact heart. The blue square shows the optical field of view (6 mm by 6 mm). *Right,* optical field of view captured through the camera and superimposed with anatomical landmarks. SVC and IVC: superior and inferior vena cava; RAA: right atrial appendage; RV and LV: right and left ventricles; PVs: pulmonary veins. (**B**) Color contour activation maps acquired with 1.0 msec (*left*) and 0.5 msec (*right*) sampling rate. On the right of each map, the corresponding color time scale indicating atrial activation time (from the earliest activation point shown in blue, to the latest activation point shown in red) is shown. The earliest atrial activation site is labeled by an asterisk. (**C**) SAN recovery time (SANRT) measured in the whole-heart preparation. Representative examples of the atrial activation contour maps reconstructed for the last pacing stimulus (S1) and for the first post-pacing atrial beat (A1) are shown for the beats selected on the representative OAP trace on top. Sites of the earliest atrial activation are labelled by an asterisk. BCL: basic cycle length. Please click here to view a larger version of this figure.

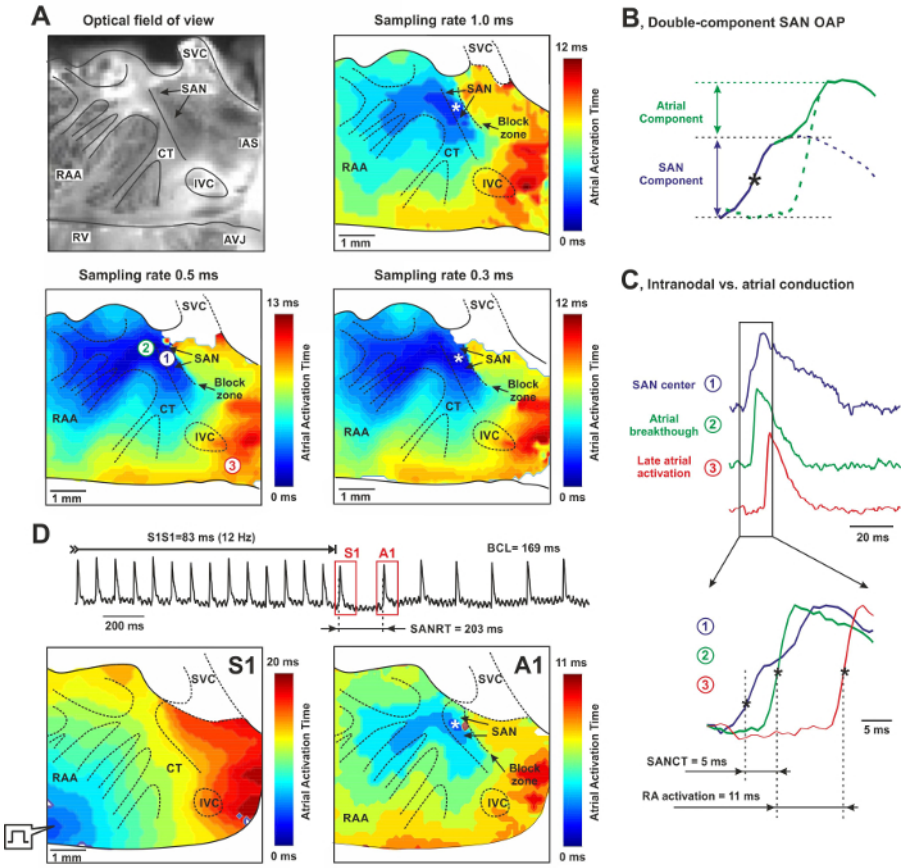

Figure 4: High-resolution Optical mapping of the Mouse Sino-atrial Node (SAN) from the Endocardial Surface of the Isolated Atria. (**A**) Photograph of a typical mouse SAN preparation (6 mm x 6 mm) and its corresponding activation contour maps obtained at 1.0 msec, 0.5 msec, and 0.3 msec sampling rates. SAN and a neighbor block zone are shown by arrows. Color time scales indicate atrial activation time. The asterisk indicates the location of the leading pacemaker. RAA: right atrial appendage, SVC and INC: superior and inferior vena cava, RV: right ventricle, AVJ: atrio-ventricular junction, CT: crista terminalis, IAS: inter-atrial septum. (**B**) Mechanism of the double components of the OAP recording from the mouse SAN area. See details in text. (**C**) OAPs recorded from the center of the SAN area (blue), the earliest atrial excitation site (green) and the latest RA activation site (red). *Insets*: transition from nodal to atrial waveform with a total conduction time equal to 5 msec. Compare it with the time delay for total RA activation equal to 11 msec. (**D**) SAN recovery time (SANRT) measured in the isolated atrial preparation. Representative examples of the atrial activation contour maps reconstructed for the last pacing stimulus (S1) and for the first post-pacing atrial beat (A1) are shown. A site of the earliest atrial activation is labeled by an asterisk. BCL - basic cycle length. Please click here to view a larger version of this figure.

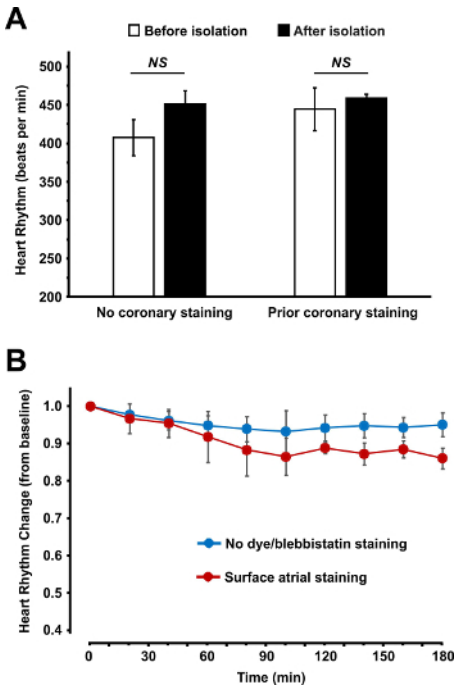

Figure 5: Heart Rhythm Measured Before and After the Atrial Isolation Procedure (**A**) and During the 3 hr Perfusion (**B**). (**A**) Spontaneous beating heart rate is shown before and after atrial isolation for two types of atrial staining: surface staining after isolation (no prior coronary staining) and coronary staining before atrial isolation. (**B**) Spontaneous beating heart rhythm stability over the 3 hr perfusion is shown for non-stained atrial preparations and for fluorescent dye and blebbistatin stained atrial preparations. Data are shown as average ± SEM. Please click here to view a larger version of this figure.

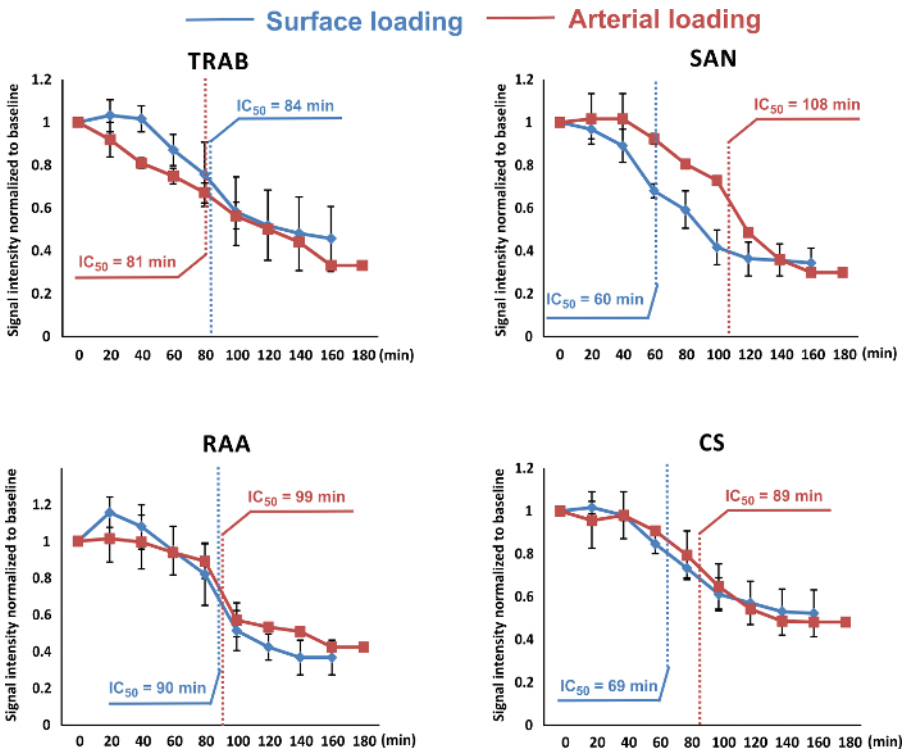

Figure 6: Signal Intensity Decay Over Time. The intensities of signals from both loading methods (coronary loading indicated in red; and surface loading indicated in blue) were measured and plotted over the time. The signal intensities were averaged from a 7 by 7-pixel area at four typical locations in the right atrium: trabecula (TRAB), sinus node (SAN), right atrium appendage (RAA) and coronary sinus (CS). IC_{50} values were then calculated and labeled in all decay curves. The signal intensity decay from both loading methods was similar in TRAB and RAA. The IC_{50} of arterial loading in CS was around 20 min longer. In the SAN, this value for arterial loading was nearly two fold larger compared to surface loading, which indicates that arterial loading methods resulted in better stability of the dye in the SAN tissue over time. Data are shown as average ± SEM. Please click here to view a larger version of this figure.

Discussion

Here, we presented two types of mouse SAN preparations: 1) intact SAN in the Langendorff-perfused whole heart, and 2) SAN in the isolated, opened atrial preparation. These two types of preparation serve different experimental purposes. In the Langendorff-perfused whole heart preparation, the intact atrial structure is preserved which makes it possible to study complex atrial arrhythmias such as atrial fibrillation as well as interactions between the SAN and atrium during reentrant tachyarrhythmias.[6] In contrast, in the isolated atrial preparation, the atrium is opened and flattened into a pseudo two dimensional structure where the three-dimensional anatomical bundles are disturbed. This may affect the anatomy of reentrant pathways which makes the isolated atrial preparation not ideal for studying atrial arrhythmogenesis. However, using this type of preparation, the location of the leading pacemaker(s) sites, intranodal conduction, and AP propagation pattern can be accurately visualized and investigated in detail. In addition, intact atria appear to be limited by a posterior view while in the isolated preparation, the entire atrial surface is available for optical mapping.

Moreover, isolated atrial preparation enables structural-functional mapping of the atrium by resolving the complex microstructure of the trabecular network as seen in **Figure 4**. For this, high spatial (100 µm/pixel or higher) and temporal (2,000 fps or higher) resolutions should be used because it is critical to particularize both atrial and SAN activation patterns, which could be further overlapped with corresponding structures. While 1,000 fps temporal resolution might be a minimum to reconstruct atrial activation (which lasts for 10 - 20 msec), 2,000 fps should be considered as a minimum temporal resolution for intranodal conduction (which lasts for ~5 ms and thus could be missed at lower resolutions) and SAN activation measurements as seen from **Figure 4**. This may allow the localization of arrhythmogenic "hot spots" (such as ectopic foci or anchored reentry) during atrial fibrillation/flutter which could emerge from the superposition of regions of significant functional remodeling with those of elevated fibrosis and/or reduced cell-to-cell coupling.[21,22] In addition, the described approach could be used to study electrophysiological mechanisms of SAN abnormalities, including SAN exit blocks, pauses, tachycardia-bradycardia arrhythmias, sick sinus syndrome *etc*.

By introducing a second (or even a third) fluorescent probe, it will be possible to perform multi-parametric optical mapping of electrical activity in association with calcium handling as well as metabolic and other changes. Different combinations of dyes could be used for simultaneous voltage-calcium, ratiometric voltage/calcium, or mitochondrial potential imaging.

For high temporal resolution optical mapping, due to the shorter fluorophore collection period, the signals of a weaker signal-to-noise ratio might be appreciated. Therefore, an averaging processing procedure is applied to the sinus heart rhythm signals or the pacing series signals as needed. The dF/dt_{max} is detected for each signal in a long period recording. These activation time points are then aligned. A setting period of recording centered at these time points is cut and averaged from all or selected Aps, as needed.

By accurate use of instrumentation and the proper staining procedure, atrial electrophysiological parameters including conduction velocity (compare **Figures 3C** and **4D** for S1 activation maps), spontaneous SAN rhythm and longevity of the SAN preparation (**Figure 5**) are not affected, which remain stable for 3 or more hours. Importantly, the continuous monitoring of ECG should be performed over the entire staining procedure to ensure normal electrical function of the heart. The application of blebbistatin may induce a transient heart rate slowing, but other than that, it does not induce any shifts in leading pacemaker sites or changes in AP morphology as was also described previously.[13]

Surface staining of the isolated atrial preparation is a critical step. For this, fast application of the diluted dye onto the surface of the tissue should be avoided; instead the dye should fall on the preparation freely due to the higher density of DMSO, which used for both dye and blebbistatin dilutions. The appropriate total loading amount and speed should be adjusted so as to not induce dramatic heart rate changes. The staining procedure could be applied several times until the signal reaches a reasonable level. It should be noted that the direct application of dye could damage the SAN tissue and affect its pacemaking. Therefore, the dye should be diluted and the amount applied should be carefully controlled. Appropriate surface staining should not damage the preparation or SAN[23] which is evaluated by comparable heart rate and conduction velocity.

Alternative staining protocols should be also considered. These can include either a 10-15 min superfusion of the SAN/atrial preparation with the voltage-sensitive dye (RH-237 or di-4-ANEPPS) at 35 ± 1°C[10,19] or a 30 min incubation of the preparation at room temperature (20-22 °C) in a Tyrode solution containing the voltage-sensitive indicator.[11]

For optical mapping of the SAN from the Langendorff-perfused whole heart, important instrumentation steps include the insertion of the small tube into the LV and the closure of SVC and IVC. The former prevents a pressure increase from solution congestion during long-term experiments as well as subsequent ischemia development after the suppression of ventricular contractions by blebbistatin and acidification of the perfusion solution. The latter enables the RA to keep some level of intra-atrial pressure thus filling the atrium with perfusion solution and flattening the intercaval region in order to uncover the entire SAN area for optical mapping.

Finally, coronary staining, in addition to surface dye loading, could significantly improve the intensity of the SAN OAPs which may last longer when compared to pure surface staining used in previous studies.[8,9]

Use of blebbistatin has multiple advantages compared to other electromechanical uncouplers including low toxicity, less pronounced side effects, and washout resistance when it is used with caution. Blebbistatin precipitates when it is dissolved at temperatures less than 37 °C.[14]Blebbistatin crystals may interrupt normal vascular flow and thus induce local ischemia and provoke arrhythmic events.[24] In addition, in studies that use GFP or other green/yellow dyes, blebbistatin precipitation could be mistaken for labeled cells which should be taken into consideration. Preventing blebbistatin precipitation is straightforward, *i.e.*, one has to dissolve blebbistatin in a pre-warmed (37 °C and higher) and vigorously stirred media.

To analyze APD, a high concentration of blebbistatin (up to 10 µM) could be used.[13,14,25]. Similarly, if any drug that increases contraction are used, additional application of blebbistatin is recommended.

As an alternative technique to study mouse SAN electrical activity, low resolution multi-electrode array (64 separate electrodes in a square 8 x 8, configuration with an inter-electrode distance of 0.55 mm)[26] and consecutive glass microelectrode recordings made at short distance between impalements[17] are used. Though those may represent relatively low-cost approaches, both have serious limitations. Multi-electrode arrays have an approximately 10-fold lower spatial resolution (they are limited by the physical size of the metal electrodes and the inter-electrode

distance and have a resolution of 550 µm/pixel *vs.* up to 50 µm /pixel for optical mapping) and cannot be used to analyze AP morphology or for multi-parametric imaging (such as simultaneous voltage and calcium optical mapping). Though glass microelectrode recordings provide more information on AP morphology, including absolute values for AP amplitude and resting potential, it is also limited by a low spatial resolution. Therefore, it can only be used for stable location of the leading pacemaker and is not applicable to capture beat-to-beat alterations in the leading pacemaker location. At the same time, as demonstrated previously[3,20] and highlighted in the present study, the SAN OAP consists of a two-phase signal whichincludes both SAN and atrial myocardium AP components (**Figure 4B**). It thus makes it difficult to extract a pure SAN signal and accurately estimate AP morphology in the SAN. For this purpose, glass microelectrodes[17] or the current clamp approach on isolated SAN myocytes should be considered.

Disclosures

No conflicts of interest are declared.

Acknowledgements

We are supported by the University of Wisconsin-Madison Medical School start-up (A.V.G.).

References

1. Efimov, I. R., Nikolski, V. P., Salama, G. Optical imaging of the heart. *Circ Res.* **95** (1), 21-33 (2004).
2. Herron, T. J., Lee, P., Jalife, J. Optical imaging of voltage and calcium in cardiac cells & tissues. *Circ Res.* **110** (4), 609-623 (2012).
3. Fedorov, V. V., Glukhov, A. V., Chang, R. Conduction barriers and pathways of the sino-atrial pacemaker complex: their role in normal rhythm and atrial arrhythmias. *Am J Physiol Heart Circ Physiol.* (2012).
4. Boyett, M. R., Honjo, H., Kodama, I. The sinoatrial node, a heterogeneous pacemaker structure. *Cardiovasc Res.* **47** (4), 658-687 (2000).
5. Glukhov, A. V. *et al.* Sinoatrial Node Reentry in a Canine Chronic Left Ventricular Infarct Model: The Role of Intranodal Fibrosis and Heterogeneity of Refractoriness. *Circ Arrhythm Electrophysiol.* (2013).
6. Glukhov, A. V. *et al.* Calsequestrin 2 deletion causes sinoatrial node dysfunction and atrial arrhythmias associated with altered sarcoplasmic reticulum calcium cycling and degenerative fibrosis within the mouse atrial pacemaker complex. *Eur Heart J.* **36** (11), 686-697 (2015).
7. John, R. M., Kumar, S. Sinus Node and Atrial Arrhythmias. *Circulation.* **133** (19), 1892-1900 (2016).
8. Swaminathan, P. D. *et al.* Oxidized CaMKII causes cardiac sinus node dysfunction in mice. *J Clin Invest.* **121** (8), 3277-3288 (2011).
9. Glukhov, A. V., Fedorov, V. V., Anderson, M. E., Mohler, P. J., Efimov, I. R. Functional anatomy of the murine sinus node: high-resolution optical mapping of ankyrin-B heterozygous mice. *Am J Physiol Heart Circ Physiol.* **299** (2), H482-491 (2010).
10. Egom, E. E. *et al.* Impaired sinoatrial node function and increased susceptibility to atrial fibrillation in mice lacking natriuretic peptide receptor C. *J Physiol.* **593** (5), 1127-1146 (2015).
11. Torrente, A. G. *et al.* Burst pacemaker activity of the sinoatrial node in sodium-calcium exchanger knockout mice. *Proc Natl Acad Sci U S A.* **112** (31), 9769-9774 (2015).
12. Lang, D., Sulkin, M., Lou, Q., Efimov, I. R. Optical mapping of action potentials and calcium transients in the mouse heart. *J Vis Exp.* (55), e3275 (2011).
13. Fedorov, V. V. *et al.* Application of blebbistatin as an excitation-contraction uncoupler for electrophysiologic study of rat and rabbit hearts. *Heart Rhythm.* **4** (5), 619-626 (2007).
14. Swift, L. M. *et al.* Properties of blebbistatin for cardiac optical mapping and other imaging applications. *Pflugers Arch.* **464** (5), 503-512 (2012).
15. Laughner, J. I., Ng, F. S., Sulkin, M. S., Arthur, R. M., Efimov, I. R. Processing and analysis of cardiac optical mapping data obtained with potentiometric dyes. *Am J Physiol Heart Circ Physiol.* **303** (7), H753-765 (2012).
16. Liu, J., Dobrzynski, H., Yanni, J., Boyett, M. R., Lei, M. Organisation of the mouse sinoatrial node: structure and expression of HCN channels. *Cardiovasc Res.* **73** (4), 729-738 (2007).
17. Verheijck, E. E. *et al.* Electrophysiological features of the mouse sinoatrial node in relation to connexin distribution. *Cardiovasc Res.* **52** (1), 40-50 (2001).
18. Krishnaswamy, P. S. *et al.* Altered parasympathetic nervous system regulation of the sinoatrial node in Akita diabetic mice. *J Mol Cell Cardiol.* **82** 125-135 (2015).
19. Nygren, A., Lomax, A. E., Giles, W. R. Heterogeneity of action potential durations in isolated mouse left and right atria recorded using voltage-sensitive dye mapping. *Am J Physiol Heart Circ Physiol.* **287** (6), H2634-2643 (2004).
20. Efimov, I. R., Fedorov, V. V., Joung, B., Lin, S. F. Mapping cardiac pacemaker circuits: methodological puzzles of the sinoatrial node optical mapping. *Circ Res.* **106** (2), 255-271 (2010).
21. Aschar-Sobbi, R. *et al.* Increased atrial arrhythmia susceptibility induced by intense endurance exercise in mice requires TNFalpha. *Nat Commun.* **6**, 6018 (2015).
22. Hansen, B. J. *et al.* Atrial fibrillation driven by micro-anatomic intramural re-entry revealed by simultaneous sub-epicardial and sub-endocardial optical mapping in explanted human hearts. *Eur Heart J.* **36** (35), 2390-2401 (2015).
23. Lang, D., Petrov, V., Lou, Q., Osipov, G., Efimov, I. R. Spatiotemporal control of heart rate in a rabbit heart. *J Electrocardiol.* **44** (6), 626-634 (2011).
24. Kanlop, N., Sakai, T. Optical mapping study of blebbistatin-induced chaotic electrical activities in isolated rat atrium preparations. *J Physiol Sci.* **60** (2), 109-117 (2010).
25. Glukhov, A. V., Flagg, T. P., Fedorov, V. V., Efimov, I. R., Nichols, C. G. Differential K(ATP) channel pharmacology in intact mouse heart. *J Mol Cell Cardiol.* **48** (1), 152-160 (2010).
26. Wu, J. *et al.* Altered sinoatrial node function and intra-atrial conduction in murine gain-of-function Scn5a+/DeltaKPQ hearts suggest an overlap syndrome. *Am J Physiol Heart Circ Physiol.* **302** (7), H1510-1523 (2012).

